

GAMMA-RAY VARIABILITY OF THE BL LACERTAE OBJECT MARKARIAN 421

J. H. BUCKLEY,¹ C. W. AKERLOF,² S. BILLER,³ D. A. CARTER-LEWIS,⁴ M. CATANESE,⁴ M. F. CAWLEY,⁵ V. CONNAUGHTON,^{1,6}
D. J. FEGAN,⁶ J. P. FINLEY,⁷ J. GAIDOS,⁷ A. M. HILLAS,³ J. F. KARTJE,⁸ A. KÖNIGL,⁸ F. KRENNRICH,⁴ R. C. LAMB,⁴
R. LESSARD,⁶ D. J. MACOMB,^{9,10} J. R. MATTOX,^{10,11} J. E. MCENERY,⁶ G. MOHANTY,⁴ J. QUINN,⁶
A. J. RODGERS,³ H. J. ROSE,³ M. S. SCHUBNEL,² G. L. SEMBROSKI,⁷ P. S. SMITH,¹²
T. C. WEEKES,¹ C. WILSON,⁷ AND J. ZWEERINK⁴

Received 1996 June 17; accepted 1996 September 9

ABSTRACT

We report on the γ -ray variability of Mrk 421 at $E_\gamma > 300$ GeV during the 1995 season, and concentrate on the results of an intense multiwavelength observing campaign in the period April 20 to May 5, which included >100 MeV γ -ray, X-ray, extreme-ultraviolet, optical, and radio observations, some of which show evidence for correlated behavior. Rapid variations in the TeV γ -ray light curve with doubling and decay times of $\lesssim 1$ day require a compact emission region and significant Doppler boosting. The TeV data reveal that the γ -ray emission is best characterized by a succession of rapid flares with a relatively low baseline level of steady emission.

Subject headings: gamma rays: observations — BL Lacertae objects: individual (Markarian 421)

1. INTRODUCTION

The Whipple 10 m air Cerenkov telescope has now detected two extragalactic sources of γ -rays above 300 GeV: Mrk 421 and Mrk 501 (Punch et al. 1992; Quinn et al. 1996). Both of these belong to the BL Lacertae class of active galactic nuclei (AGNs), which is a subset of the broader blazar class, and have a number of similar properties (Weekes et al. 1996). Gamma-ray variability (on a timescale of days) has been previously observed for both sources (Kerrick et al. 1995; Quinn et al. 1996).

Although there is no universal consensus on the origin of the nonthermal continuum emission characteristic of blazars, it is widely believed that, from the radio through the UV wave bands (or even X-ray wave bands for some objects), the bulk of their emission is beamed, incoherent, synchrotron radiation from relativistic jets that are observed at small angles to their axes (e.g., Blandford & Rees 1978). Above the presumed synchrotron break, a second high-energy component is often observed in the X-ray or γ -ray wave band (von Montigny et al. 1995). A number of mechanisms have been proposed to explain the high-energy X-ray or γ -ray emission, including synchrotron self-Compton emission (e.g., Königl 1981), Compton up-scattering of external

accretion disk photons (Melia & Königl 1989; Dermer, Schlickeiser, & Mastichiadis 1992; Sikora, Begelman, & Rees 1994), or pair cascades produced by high-energy protons or electrons (Sikora et al. 1987; Mannheim 1993; Coppi, Kartje, & Königl 1993). The relative amplitudes and timescales of variability at different wavelengths and the presence of correlations between these data impose important constraints on these models.

Observations made in 1994 indicate a possible coincidence of a high X-ray state and a TeV flare on 1994 May 15, with a coincidence window of ~ 10 days (Takahashi et al. 1994; Kerrick et al. 1995). To obtain a better measure of its variability timescale and to better overlap with multiwavelength observations, Mrk 421 was extensively observed throughout the 1995 season by the Whipple Observatory's 10 m γ -ray telescope. In § 2, the Whipple γ -ray telescope and the imaging Cerenkov technique are described. The results of these observations are given in § 3, together with a comparison to optical, extreme-UV, and X-ray observations. The implications of these observations are discussed briefly in § 4.

2. GAMMA-RAY OBSERVATIONS

The high-energy γ -ray telescope (Cawley et al. 1990) at the Whipple Observatory employs a 10 m diameter optical reflector to image Cerenkov light from air showers onto an array of 109 fast photomultipliers (PMT) covering a 3° field of view. By making use of the distinctive differences in the angular distribution of light and orientation of the shower images, a γ -ray signal can be extracted from the large background of hadronic showers (Reynolds et al. 1993). The details of the data analysis are described elsewhere (e.g., Quinn et al. 1996). The brightness level in each PMT is also monitored, giving the position of stars in the focal plane to an accuracy of $\lesssim 0.04^\circ$. For Mrk 421, two stars (SAO 62387 and SAO 62392) near the center of the field of view provide an online check of the pointing to ensure that pointing errors do not result in artificial variations in the observed flux of Mrk 421.

To check the stability of the technique by which γ -ray rates are derived, we have analyzed our observations of the Crab

¹ Fred Lawrence Whipple Observatory, Harvard-Smithsonian CfA, P.O. Box 97, Amado, AZ 85645-0097.

² Randall Laboratory of Physics, University of Michigan, Ann Arbor, MI 48109-1120.

³ Department of Physics, University of Leeds, Leeds, LS2 9JT, Yorkshire, England, UK.

⁴ Department of Physics and Astronomy, Iowa State University, Ames, IA 50011-3160.

⁵ Physics Department, St. Patrick's College, Maynooth, County Kildare, Ireland.

⁶ Physics Department, University College, Dublin 4, Ireland.

⁷ Department of Physics, Purdue University, West Lafayette, IN 47907.

⁸ Department of Astronomy and Astrophysics, University of Chicago, Chicago, IL 60637.

⁹ Laboratory for High-Energy Astrophysics, NASA/GSFC, Greenbelt, MD 20771.

¹⁰ Astrophysics Program, Universities Space Research Association.

¹¹ Astronomy Department, University of Maryland, College Park, MD 20742.

¹² Steward Observatory, University of Arizona, Tucson, AZ 85721.

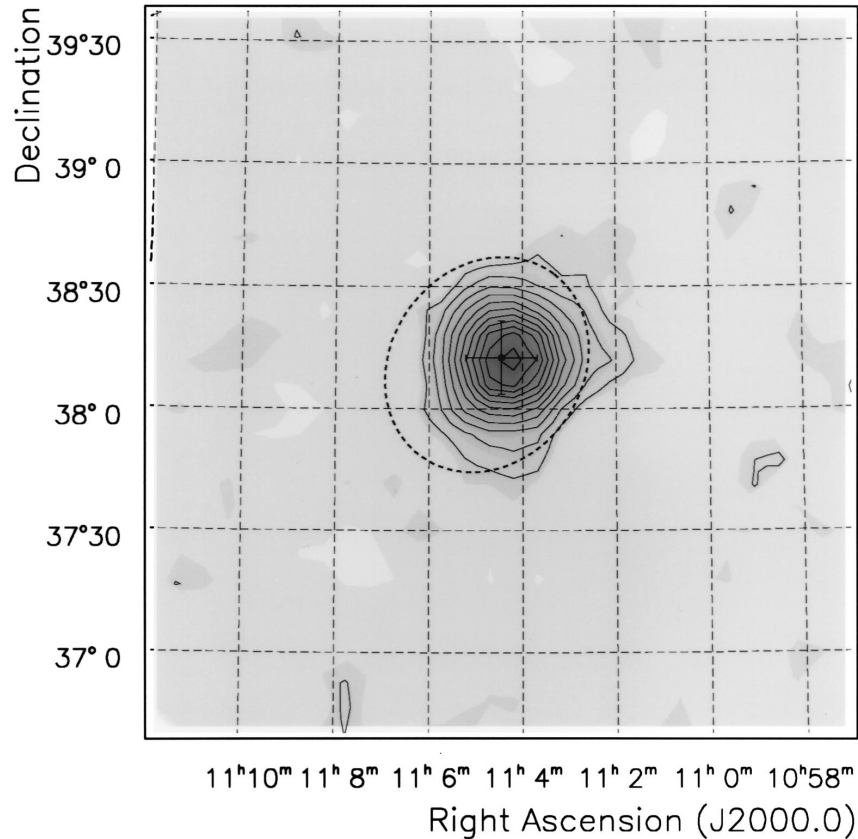


FIG. 1.—Two-dimensional plot of the γ -ray emission from the region around Mrk 421. The gray scale is proportional to the number of excess counts (or number of γ -rays) consistent with each mesh point, and the solid contours correspond to 2σ levels derived from the likelihood ratio statistic. The dashed ellipse gives the 95% confidence interval determined by EGRET (Thompson et al. 1995). The derived position of Mrk 421 (after a pointing correction) is indicated by the cross.

Nebula taken during the last two observing seasons on a night-by-night basis. If no systematic errors are present and if the emission from the Crab Nebula is steady, then the normalized γ -ray rates for individual Crab runs, given by $(r_i - \langle r \rangle) / \sigma_r^i$ (where $\langle r \rangle$ is the average count rate and σ_r^i is the statistical uncertainty in the measured rate r_i), should be normally distributed with unit variance. The actual distribution of Crab fluxes has a width of $\sigma = 1.0 \pm 0.1$, indicating that the level of systematic errors associated with the variations seen in Mrk 421 is small in comparison with statistical errors.

3. RESULTS

Figure 1 shows the two-dimensional map of excess events for 26 hr of on-source data and 26 hr of off-source (control) data, for which the total significance of the detection was 23σ . This method is based closely on that of Akerlof et al. (1991), with minor modifications described in more detail by Lessard & Buckley (1996). Contours of the statistic $S = (-2 \ln \lambda)^{1/2}$ (where λ is the likelihood ratio derived from the on- and off-source counts at a given grid point) are shown in 2σ increments. The first and second contours from the center correspond to the 68% and 99.7% confidence intervals, respectively. The cross represents the pointing-corrected position of Mrk 421. Also shown, as the dashed contour, is the elliptical fit to the EGRET 95% confidence interval. The identification of the Whipple γ -ray source with Mrk 421 is fairly certain, and is further strengthened by the multiwavelength correlations described below.

Figure 2 shows the daily γ -ray rates for observations taken on 62 days in 1995. These data indicate that daily observations

undersample the most rapid variability in the light curve. On a number of occasions doubling times and decay times of ≈ 1 day are apparent (e.g., MJD 49,832–49,833 and MJD 49,830–49,831, respectively), and a longer timescale of the order of ~ 1 week can be seen in the light curve. The data suggest that the γ -ray emission is best characterized by a succession of rapid flares with a baseline level near the sensitivity limit and consistent with little steady emission.

Observations in a number of different wave bands taken between 1995 April 20 and May 17 are shown in Figure 3. The 0.7–7.5 keV X-ray flux measured by the *Advanced Satellite for*

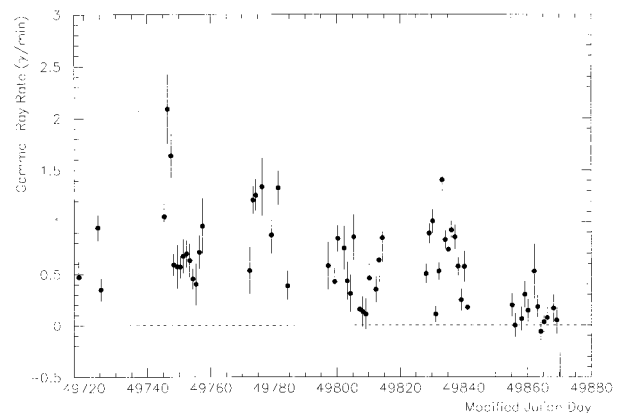


FIG. 2.—Daily γ -ray rates at $E > 300$ GeV for Mrk 421 during the 1995 season.

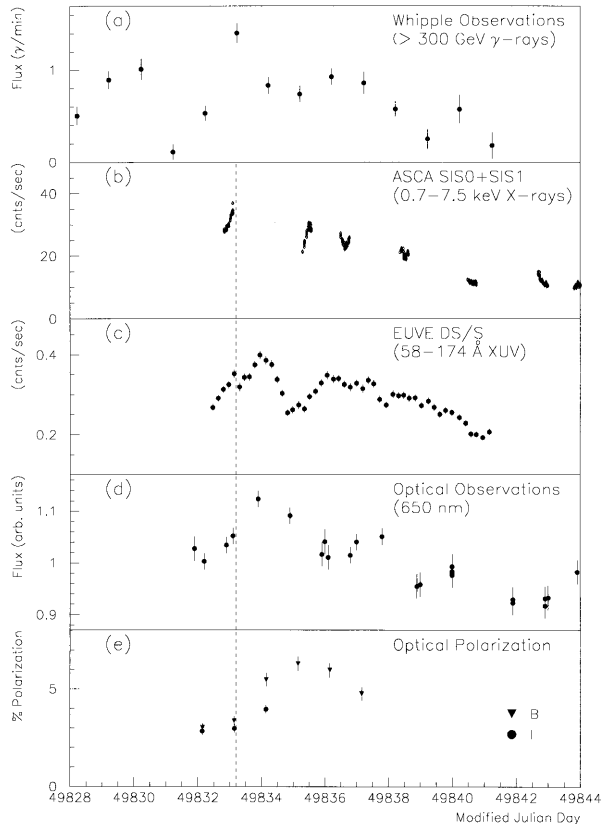


FIG. 3.—(a) Gamma-ray, (b) X-ray (Takahashi et al. 1996), (c) extreme-UV (Kartje et al. 1996), and (d) optical (Wagner et al. 1996) light curves for Mrk 421 taken during the 1995 April–May multiwavelength campaign. (e) Optical polarization measurements in the *B* and *I* band taken during the same period. Note that 1995 April 26 corresponds to MJD 49,833.

Cosmology and Astrophysics (ASCA) drops from a peak value of 2.3×10^{-10} ergs cm^{-2} s^{-1} to 0.4×10^{-10} ergs cm^{-2} s^{-1} (Takahashi 1996). These data and the TeV γ -ray data both indicate a doubling time of ~ 1 day and a decline on a timescale of ~ 1 week. Extreme-ultraviolet data taken during this period with the *Extreme-Ultraviolet Explorer (EUVE)* Deep Survey Spectrometer (DS/S) (spanning the wavelength interval 58–174 Å) show a clear correlation of the detailed shape of the light curve with the γ -ray data, but have a smaller variability amplitude than the X-ray data. Simultaneous observations taken during the period April 24–May 17 in the optical band (650 nm) shown in Figure 3d (Wagner 1996) also indicate a correlation with the γ -ray data, but the amplitude of the variations (after a subtraction of the background galaxy light) are of the order of $\sim 20\%$, much smaller than the variations at shorter wavelengths. The optical variability time-scales are also apparently somewhat longer.

Figure 3e shows optical polarization data taken with the Two-Holer polarimeter on the Steward Observatory 1.55 m telescope using a 9" aperture centered on the nucleus of Mrk 421. No galaxy light subtraction has been performed for this measurement. The peak polarization at 6% in the blue is near the maximum reported previously for Mrk 421. These data indicate a color-dependent lag in the polarization, as well as increasing polarization at shorter wavelengths.

Radio data taken with the University of Michigan 26 m telescope (Aller & Aller 1995) indicate a 14.5 GHz radio flux of 0.58 ± 0.02 Jy on 1995 April 29, lower than the measured

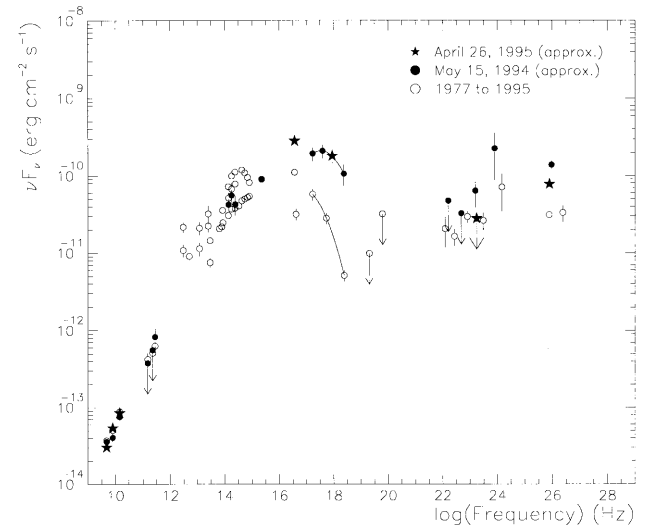


FIG. 4.—Multiwavelength spectrum of Mrk 421 from data taken over the period 1977–1994 (*open circles*), within a few days of the 1994 May 15 flare (*filled circles*) and during the 1995 April 26 flare (*stars*).

value of 0.65 ± 0.01 on 1995 March 14. The flux measured on 1994 May 14 (1 day prior to the TeV flare reported in Kerrick et al. 1995) was 0.52 ± 0.02 (Macomb et al. 1995).

EGRET observations were also made during this period, but did not result in a positive detection of Mrk 421. Using the data taken with a 1.3×10^8 cm^2 s exposure over the period 1995 April 25–May 9, the significance level for $E > 100$ MeV is 0.3σ with a 2σ upper limit of 1.2×10^{-7} cm^{-2} s^{-1} .

Given the undersampled light curves, we do not try to quantify precisely the time lag between various measurements, but can obtain a rough measure of the significance of the correlation and time lag using the discrete correlation function (DCF) defined in Edelson & Krolik (1988), which is appropriate for unevenly sampled data. Cross-correlations of the various data sets indicate a significant correlation of the X-ray and γ -ray data with no time lag, and a maximum correlation when a shift of ~ 1 day is introduced to both the *EUVE* and optical data relative to the X-ray/ γ -ray emission.

In view of the rapid, large-amplitude variability of Mrk 421 in many wave bands, a meaningful multiwavelength spectrum can only be formed using nearly simultaneous data. Figure 4 shows this spectrum for the two periods where roughly simultaneous measurements were made.

The stars show the data taken within two days of the flare on 1995 April 26. The TeV flux from this day is calculated using an effective area of 3.0×10^8 cm^2 and median γ -ray energy of 330 GeV, and is converted to a differential point assuming an $E^{-2.7}$ spectrum. The X-ray flux point at 1.8×10^{-10} ergs cm^{-2} s^{-1} is the average value for observations taken over 1995 April 25.8–26.1 UT given in Takahashi et al. (1995). Also shown is the average *EUVE* flux on the day of the flare of approximately 2.8×10^{-10} ergs cm^{-2} s^{-1} at $\lambda \approx 80$ Å assuming a value of $N_{\text{H}} = 1.45 \times 10^{20}$ cm^{-2} for the Galactic hydrogen column density (Elvis, Lockman, & Wilkes 1989), with a spectral slope of $\alpha \approx 1.3$ joining the *EUVE* and 1.5 keV *ASCA* points (Kartje et al. 1996). Radio observations taken on 1995 April 29 (at 14.5 GHz), May 16 (at 8.0 GHz), and May 20 (at 4.8 GHz) by the University of Michigan 26 m telescope (Aller & Aller 1995) are also shown.

The filled circles give the data from a few days around the TeV flare on 1994 May 15, with the radio to soft-UV data as

well as the EGRET points taken from Macomb et al. (1995) and the X-ray spectrum from Macomb et al. (1996). The TeV point is derived from the integral flux which is recalculated using the same (high-threshold) cuts as applied to the 1995 data and resulting in a higher median energy of 390 GeV (due to differences in the PMT gains in the 1994 season) and the same effective area of $3.0 \times 10^8 \text{ cm}^2$.

For reference, the open circles show data taken over the extended period of 1977–1994. The radio, UV, and X-ray data are based on observations taken in 1993–1994 before the 1994 May 15 flare from Macomb et al. (1995). Two *EUVE* points are also shown, the higher of the two from data taken on 1994 April 2–12 (Fruscione et al. 1996) and the lower from data taken during the *EUVE* all-sky survey (Marshall, Fruscione, & Carone 1995). For the all-sky survey data, a flux of $3.2 \pm 0.6 \times 10^{-11} \text{ ergs cm}^{-2} \text{ s}^{-1}$ at 74 Å is derived, assuming the same spectral index and Galactic hydrogen column as given in Kartje et al. (1996) for the 1995 April data. The TeV flux is derived from the average flux as measured over the entire 1995 season and converted to a differential point as described above. Also shown is the High-Energy Gamma-Ray Array TeV flux measurement made in the 1994–1995 season (Petty et al. 1996). This compilation also includes far-infrared data taken with *IRAS* (Impey & Neugebauer 1988) and near-IR-to-optical data from Macomb et al. (1995), Makino et al. (1987) and Cruz-Gonzalez & Huchra (1984). Upper limits at $E > 50 \text{ keV}$ are derived from OSSE observations (McNaron-Brown et al. 1995).

4. DISCUSSION

Observations of the γ -ray flux of Mrk 421 show dramatic variability, with the emission characterized by day-scale flickering and with no well-defined steady component. The measurements of the γ -ray light curves made with the Whipple Observatory telescope have a comparable signal-to-noise ratio to those obtained for the brightest blazars by any instrument on the *Compton Gamma-Ray Observatory*, and provide important new data for testing blazar emission models. The rapid

variability and high energy of these γ -rays imply compact emission regions and require significant Doppler boosting to lower the predicted high opacities from γ - γ pair production. If the correlations of the optical to UV emission imply that they are produced in the same emission region as the TeV radiation, then the lower limit on the relativistic Doppler factor of this region is given by $\delta \gtrsim 4.9(\tau/10^5 \text{ s})^{-1/5.4}(F_U/10 \text{ mJy})^{1/5.4}$, where τ is the doubling time and F_U is the optical *U* band flux (Mattox et al. 1993; Buckley 1996). In contrast to the prediction of some unified models that X-ray-selected BL Lac objects (XSBLs) are viewed at relatively large angles to their jet axes, it appears that Mrk 421, and perhaps other XSBLs such as Mrk 501, may have relatively large Doppler factors. The absence of emission-line clouds in BL Lac objects could also reduce the opacity from ambient photons and explain why TeV emission is seen in these objects but not other nearby AGNs (Dermer & Schlickeiser 1994). Still, the compactness implied by the short variability timescales of the TeV emission presents a major challenge for most BL Lac emission models (Sikora et al. 1994; Königl 1994).

Correlations between the X-ray and TeV γ -ray emission and the short variability timescales imply that both components may be produced by the same population of electrons, with the X-rays at the endpoint of the synchrotron spectrum and the γ -rays near the endpoint of an inverse Compton spectrum. With the detection of Mrk 421 and Mrk 501 in TeV γ -rays, it is possible that in other X-ray-selected objects the extension of the synchrotron emission into the X-ray wave band signals the emission of $\gtrsim \text{TeV}$ photons, and is as important as the effect of intrinsic absorption (Dermer & Schlickeiser 1994) or intergalactic absorption (Stecker, de Jager & Salamon 1993) on the observability of AGNs at TeV energies.

We wish to thank M. F. Aller and H. D. Aller for making their radio observations available, and S. Wagner and P. Coppi for useful discussions. This research is supported by grants from the US Department of Energy and by NASA, by PPARC in the UK, and by Forbairt in Ireland.

REFERENCES

- Akerlof, C. W., et al. 1991, *ApJ*, 377, L97
 Aller, H. D., & Aller, M. F. 1995, private communication
 Blandford, R. D., & Rees, M. J. 1978, in *Proc. Pittsburgh Conference on BL Lac Objects*, ed. A. N. Wolfe (Pittsburgh: Univ. Pittsburgh Press), 328
 Buckley, J. H. 1996, in preparation
 Cawley, M. F., et al. 1990, *Exp. Astron.*, 1, 173
 Coppi, P. S., Kartje, J. F., & Königl, A. 1993, in *Proc. Compton Symposium*, ed. M. Friedlander, N. Gehrels, & D. J. Macomb (New York: AIP), 559
 Cruz-Gonzalez, I., & Huchra, J. P. 1984, *AJ*, 89, 441
 Dermer, D., & Schlickeiser, R. 1994, *ApJS*, 90, 945
 Dermer, D., Schlickeiser, R., & Mastichiadis, A. 1992, *A&A*, 256, L27
 Edelson, R., et al. 1995, *ApJ*, 438, 120
 Edelson, R. A., & Krolik, J. H. 1988, *ApJ*, 333, 646
 Elvis, M., Lockman, F. J., & Wilkes, B. J. 1989, *AJ*, 97, 777
 Fruscione, A., et al. 1996, in *Proc. 11th Colloq. on UV and X-Ray Spectroscopy of Astrophysical and Laboratory Plasmas*, in press
 Impey, C. D., & Neugebauer, G. 1988, *AJ*, 95, 2
 Jones, T. W., O'Dell, S. L., & Stein, W. A. 1974, *ApJ*, 188, 353
 Kartje, T., et al. 1996, in preparation
 Kerrick, A. D., et al. 1995, *ApJ*, 438, L59
 Königl, A. 1981, *ApJ*, 243, 700
 ———. 1994, in *ASP Conf. Ser. 54, Proc. First Stromlo Symposium: The Physics of Active Galaxies*, ed. G. V. Bicknell, M. A. Dopita, & P. J. Quinn (San Francisco: ASP), 33
 Lessard, R. W., & Buckley, J. H. 1996, in preparation
 Li, T. P., & Ma, Y. Q. 1983, *ApJ*, 272, 317
 Macomb, D. J., et al. 1995, *ApJ*, 449, L99
 ———. 1996, *ApJ*, 459, L111
 Makino, F., et al. 1987, *ApJ*, 313, 662
 Mannheim, K. 1993, *A&A*, 269, 67
 Marshall, H. L., Fruscione, A., & Carone, T. E. 1995, *ApJ*, 439, 90
 Mattox, J. R., et al. 1993, *ApJ*, 410, 609
 Maza, J., Martin, P. G., & Angel, J. R. P. 1978, *ApJ*, 224, 368
 McNaron-Brown, K., et al. 1995, *ApJ*, 451, 575
 Melia, F., & Königl, A. 1989, *ApJ*, 340, 162
 Petty, D., et al. 1996, *A&A*, in press
 Punch, M., et al. 1992, *Nature*, 358, 477
 Quinn, J., et al. 1996, *ApJ*, 456, L83
 Reynolds, P. T., et al. 1993, *ApJ*, 404, 206
 Sikora, M., et al. 1987, *ApJ*, 320, L81
 Sikora, M., Begelman, M. C., & Rees, M. J. 1994, *ApJ*, 421, 153
 Stecker, F. W., de Jager, O. C., & Salamon, M. 1993, *ApJ*, 415, L71
 Takahashi, T. 1996, *Mem. Soc. Astron. Italiana*, in press
 Takahashi, T., et al. 1994, *IAU Circ.* 5993
 ———. 1995, *IAU Circ.* 6167
 Thompson, D. J., et al. 1995, *ApJS*, 101, 259
 von Montigny, C., et al. 1995, *ApJ*, 440, 525
 Wagner, S. 1996, *ApJ*, submitted
 Weekes, T. C., et al. 1996, *A&A*, in press